



OPEN

Acupuncture modulates cortical thickness and functional connectivity in knee osteoarthritis patients

SUBJECT AREAS:

TRANSLATIONAL
RESEARCH

OUTCOMES RESEARCH

Xiaoyan Chen, Rosa B. Spaeth, Kallirroi Retzepi, Daniel Ott & Jian Kong

Received
30 June 2014Accepted
2 September 2014Published
26 September 2014Correspondence and
requests for materials
should be addressed to
J.K. (kongj@nmr.mgh.
harvard.edu)

Department of Psychiatry, Massachusetts General Hospital, Charlestown, MA, USA.

In this study, we investigated cortical thickness and functional connectivity across longitudinal acupuncture treatments in patients with knee osteoarthritis (OA). Over a period of four weeks (six treatments), we collected resting state functional magnetic resonance imaging (fMRI) scans from 30 patients before their first, third and sixth treatments. Clinical outcome showed a significantly greater Knee Injury and Osteoarthritis Outcome Score (KOOS) pain score (improvement) with verum acupuncture compared to the sham acupuncture. Longitudinal cortical thickness analysis showed that the cortical thickness at left posterior medial prefrontal cortex (pMPFC) decreased significantly in the sham group across treatment sessions as compared with verum group. Resting state functional connectivity (rsFC) analysis using the left pMPFC as a seed showed that after longitudinal treatments, the rsFC between the left pMPFC and the rostral anterior cingulate cortex (rACC), medial frontal pole (mFP) and periaquiduct grey (PAG) are significantly greater in the verum acupuncture group as compared with the sham group. Our results suggest that acupuncture may achieve its therapeutic effect on knee OA pain by preventing cortical thinning and decreases in functional connectivity in major pain related areas, therefore modulating pain in the descending pain modulatory pathway.

Osteoarthritis (OA) is a major public health problem among the elderly and is associated with considerable disability¹. The knee is one of the most common body locations for OA. A recent analysis of data from the National Health and Nutrition Examination Survey III (NHANES III) indicated that about 35% of women and men aged 60 years and above had radiographic knee OA².

OA is a complex chronic pain condition due in part to both nociceptive and neuropathic mechanisms³. Previous studies have demonstrated central sensitization in osteoarthritis patients^{4–6}, increased activity in the periaqueductal grey (PAG) matter associated with stimulation of the skin in referred pain areas of patients⁶, and increased regional cerebral blood flow (rCBF) in pain related brain regions including the primary and secondary somatosensory, insula, cingulate cortices, thalamus, amygdala, hippocampus and PAG⁷, indicating pathology of the central nervous system in knee OA patients.

Despite the high prevalence rate of OA, the treatment of OA is far from satisfactory^{8,9}. Pharmacological treatment of knee OA is often ineffective with unwanted and dangerous side effects^{9,10}. Acupuncture is a component of the “Traditional Chinese Medicine” (TCM) system. Multiple randomized clinical trials have suggested that knee OA patients can benefit from acupuncture treatment^{9,11–13}. However, the mechanisms underlying the effects of acupuncture treatment in knee OA patients are still poorly understood.

As a unique treatment modality, studies have shown that acupuncture may produce an analgesic effect through the endogenous descending pain modulatory system^{14–16}. Brain imaging studies have also shown that acupuncture needle stimulation^{17–21} can evoke widespread brain activity changes and modulate the functional connectivity (FC) of the pain processing network^{22–29}, which opens a new window to understand the central mechanism of acupuncture treatment.

In parallel, investigators have found abnormal brain structures^{30–37} or disrupted FC^{36–42} in patients with various chronic pain disorders.

More recently, accumulating evidence suggest that the disrupted brain structure and functional connectivity can be reversed after successful treatment. For instance, Seminowicz and colleagues⁴³ found that cLBP is associated with decreased cortical thickness and abnormal activity during attention-demanding tasks in the dorsal lateral prefrontal cortex (DLPFC). Most intriguingly, after successful treatment of back pain, both cortical thickness and functional connectivity (FC) of the DLPFC were normalized. In another study, the investigators⁴⁴ found that gray matter volume decreases within the left thalamus in patients with osteoarthritis of the hip; these

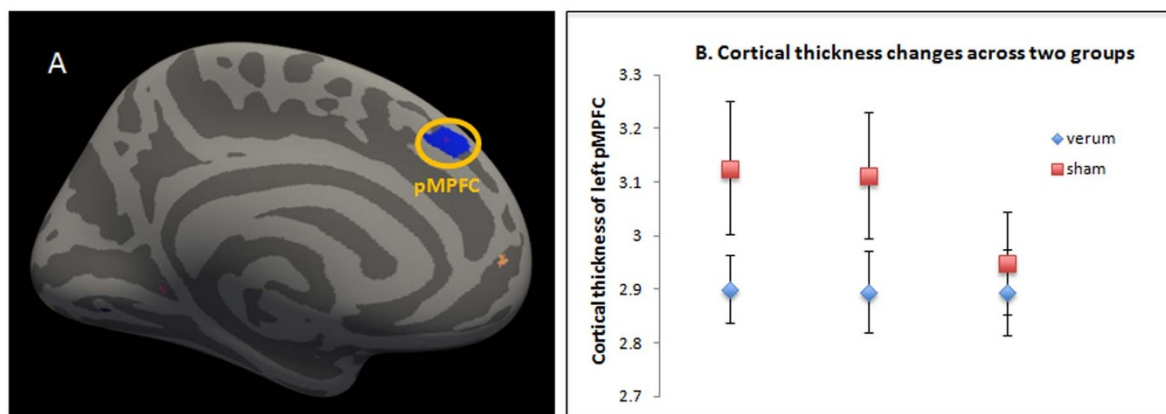


Figure 1 | Structural changes after longitudinal treatments (A) The cortical thickness of the left posterior MPFC showed significant interaction between verum and sham groups across three treatment sessions (B) The cortical thickness of left posterior MPFC in sham group decreases across treatment sessions (baseline, week 1 and week 4), while that of verum group stays roughly the same.

thalamic volume changes reverse after hip arthroplasty and are associated with decreased pain and increased function.

In the present study, we investigated changes in cortical thickness and functional connectivity in knee OA patients across longitudinal acupuncture treatments. All patients were randomized to receive either verum or sham acupuncture. Using a longitudinal treatment design⁹, each patient received 6 acupuncture treatments over 4 weeks. We collected brain structure and resting state functional magnetic resonance imaging (fMRI) scans during the first, third and sixth treatments (Supplemental Figure 1a). We also administered the Knee Injury and Osteoarthritis Outcome Score (KOOS)⁴⁵ before and after the six-session acupuncture treatment period.

Methods

Subjects. The Institutional Review Board at Massachusetts General Hospital approved all study procedures. The experiment was performed in accordance with approved guidelines. All subjects who enrolled in this study provided written informed consent before beginning any study procedure. We debriefed all subjects at the end of the study.

Patient recruitment and inclusion criteria. We recruited acupuncture naïve patients aged 40–70 with a diagnosis of chronic osteoarthritis (OA) in the right and/or left knee from Massachusetts General Hospital (MGH), Brigham and Women's Hospital (BWH) and the greater Boston area.

Subjects exhibiting Grade 2 or Grade 3 OA as defined by the Kellgren-Lawrence Scale used for radiographically grading knee OA were included in the study. We excluded subjects who: 1) had undergone any interventional procedures for knee pain within 6 months prior to enrolling in the study, 2) intended to undergo surgery during the time of involvement in the study, 3) experienced knee pain due to causes other than OA, such as inflammation or malignancy, 4) had received a diagnosis of rheumatoid arthritis or other leg-related pain disorders, 5) were taking opioids, benzodiazepines, or other medications that may influence brain imaging outcomes, or 6) presented MRI contraindications. All enrolled OA patients had an endogenous average pain intensity rating of >2 on the Brief Pain Inventory (BPI) scale at the first visit.

Experimental design. All subjects, regardless of the presence of bilateral or unilateral pain, received treatment on the knee that presented them with the most severe pain. We stratified subjects by knee and randomized them into one of three groups: high dose real acupuncture (6 acupoints), low dose real acupuncture (2 acupoints), or high dose sham acupuncture (6 non-acupoints with Streitberger placebo needles) (Supplemental Figure 1b). Subjects were randomized using a block design generated by a biostatistician blind to the treatment mode. Only the acupuncturist was not blinded. This study was designed to investigate whether the number of needles (acu points) influences the treatment effect. Therefore, we included two groups receiving real acupuncture treatments with different numbers of acu points, but identical stimulation paradigm.

After an initial screening session, each subject engaged in a total of 6 acupuncture treatment sessions in one month (twice per week for the first two weeks, once per week for the last two weeks). Treatments 1, 3 and 6 occurred during a scan session with the patient lying in a 3-Tesla MRI scanner while we acquired fMRI data. All other treatments occurred in our behavioral testing room.

Acupuncture administration. Each acupuncture treatment session lasted about 25 minutes for subjects in both the verum and sham acupuncture groups. The two acupoints selected for the low dose acupuncture group (ST35 and Xi yan (extra point)) were located near the knee. Each acupoint was stimulated a total of twelve times. The high dose acupuncture group received treatment at four additional acupoints (GB34, SP9, GB39 and SP6) (see Supplemental Figure 1c) and each acupoint was stimulated 4 times. The locations of all acupoints were based on the text book of Chinese Acupuncture⁴⁶. All these points are well documented for the treatment of knee pain^{9,11,12}.

For subjects receiving sham acupuncture, the acupuncturist applied placebo needles^{47–50} at six non-acupoints using a paradigm identical to that of the high dose verum needle administration. Rather than penetrating the skin as a verum needle does, the sham needle retracts up the handle shaft when the acupuncturist presses it against the skin. Sham point 1 was located 1.5 cun posterior and inferior to GB4, sham points 2–3 were located 1.5 cun and 3 cun inferior to sham point 1, sham point 4 was located 1 cun posterior to the midpoint of K9 and K10, and sham 5–6 were located 1.5 cun inferior and superior to the sham point 4 respectively. All sham points were located on the lower leg where no meridians pass (Supplemental Figure 1c).

For all treatments, the acupuncturist placed a small plastic ring over the point and secured the ring with a thin strip of sterile plastic tape ensuring patient blindness to the actual site of needle insertion and thus blindness to whether the treatment was verum or sham. During acupuncture, the acupuncturist stimulated one point at a time in a predetermined order, each for 10 seconds with 30-second breaks between each acupoint. (Supplemental Figure 1a). The total treatment and stimulation time for all three groups was the same. We randomized the specific starting acupoint across patients, but held it constant throughout all sessions for each individual patient. For consistency, we kept leg position, acupoint location, and needling parameters (1–2 cm depth for all points, all needles were evenly rotated approximately 120 rotations per minute, we also attempted to produce moderate deqi sensations on a 0–10 scale) constant across groups. In the fMRI sessions, the treatment spanned two 9-minute acupuncture/fMRI scans followed by Massachusetts General Hospital Acupuncture Sensation Scale (MASS) rating.

As a treatment quality control, we measured the deqi sensation evoked by two separate acupuncture stimulation periods, one midway through the treatment and one at the end of the treatment, using the MASS^{51,52}.

Clinical outcomes. We measured clinical outcomes using the KOOS⁴⁵, which is comprised of 5 subscales: 1) pain, 2) other symptoms, 3) function in daily living (ADL), 4) function in sport and recreation, and 5) knee-related quality of life (QOL). Each subscale allows for calculation of a normalized score, with 0 denoting the most extreme symptoms/pain and 100 denoting no symptoms/pain⁴⁵. Based on previous studies⁹, we selected the KOOS pain subscale and function in daily living subscale as our primary outcome measures. We used all other subscale measurements as secondary outcomes. Trained research assistants, blinded to treatment mode, administered the KOOS to all patients at baseline (up to one week prior to the first treatment) and again after the final treatment.

fMRI data acquisition. Each subject participated in three identical fMRI scanning sessions. Scan 1 (treatment 1) and scan 2 (treatment 3) were separated by approximately 7 days; scan 2 and scan 3 (treatment 6) were separated by approximately 18 days. We used a 3-axis gradient head coil in a 3-Tesla Siemens MRI system equipped for echo planar imaging (EPI). Each fMRI session included an anisotropic magnetization prepared rapid gradient-echo (MPRAGE) structural sequence followed by a 6-minute resting state fMRI. The MPRAGE scanning parameters included TR of 2200 ms, echo time of 9.8 ms, flip angle of 7°, field-of-view of 230 mm², slice thickness of 1.2 mm. For the resting state, the scan acquisition included 47 slices with a thickness of 3 mm, a TR of 3000 ms, a TE of 30 ms, flip angle



of 85 degrees, field of view of 216 mm² and a 3 × 3-mm in-plane spatial resolution. Following the first resting state fMRI, we conducted two functional scans during the 25-minute acupuncture administration and a second resting state scan following acupuncture administration (Supplemental Figure 1a).

Data analysis. Brain structure analysis using FreeSurfer. Automated cortical surface reconstruction was performed on the T1 MPRAGE scans in FreeSurfer version 5.1 (<http://surfer.nmr.mgh.harvard.edu>) using previously described methods^{53–55}. FreeSurfer's Longitudinal Processing Stream⁵⁶ was used to analyze the cortical changes between groups. The longitudinal processing stream creates an unbiased within-subject template space and image⁵⁷ using robust, inverse consistent registration⁵⁸. The template is used as an estimate to initialize subsequent segmentation processes for each time point, providing within-subject common information regarding anatomical structures. Several processing steps, such as skull stripping, Talaraich transforms, atlas registration as well as spherical surface maps and parcellations are then initialized with common information from this template, something which significantly increases reliability and statistical power⁵⁶.

Here, the unbiased template was created for each subject using the three T1 MPRAGE scans collected over the course of one month. Any inaccuracies in the reconstruction of white matter and pial surfaces of individual subjects were visually inspected using the template reconstruction. Any inaccuracies identified by visual inspection were manually corrected on the template and applied to each of the three longitudinal scans. Cortical thickness was then computed for each longitudinal scan as the distance between the pial and white matter surfaces at each point across the cortical mantle.

Group analyses were performed by resampling each subject's data to the FreeSurfer average atlas, distributed as a part of the FreeSurfer software package. A standard General Linear Model (GLM) was used to compare the rate of change of cortical thickness between the verum and sham groups at each point across the cortical mantle.

Similar to our previous studies^{36,37}, we used an initial uncorrected threshold of $p < 0.005$ and smoothed with a Gaussian kernel with a FWHM of 10 mm in group analysis. A threshold of corrected p values ($p \leq 0.05$) as obtained by using a Monte Carlo simulation cluster-wise correction with 10000 permutations was further applied.

After computing the cortical thickness of the left posterior medial prefrontal cortex (pmPFC) for all 30 patients, repeated measurements were done to test for interactions between acupuncture mode (verum vs. sham) and time (across all three treatment sessions) using SPSS 18.0 Software (SPSS Inc., Chicago, IL, USA). To eliminate the effect of possible confounding factors, the analysis was repeated using age and duration as covariates of no interest.

Seed based functional connectivity analysis. The fMRI data were preprocessed using Data Processing Assistant for Resting-State fMRI (DPARSF) software (available at: <http://rfmri.org/DPARSF>)^{59,60} implemented in a MATLAB suite (Mathworks, Inc, Natick, Massachusetts). The software is based on Statistical Parametric Mapping (SPM8) (<http://www.fil.ion.ucl.ac.uk/spm>) and Resting-State fMRI Data Analysis Toolkit (<http://www.restfmri.net>)⁶¹.

The fMRI images were slice timing corrected, head-motion corrected, coregistered to respective structural images for each subject, segmented, regressed out 6 rigid body motion, white matter, and CSF signal, normalized by using structural image unified segmentation, and then re-sampled to 3-mm cubic voxels. After linear detrending, data was filtered using typical temporal bandpass (0.01–0.08 Hz) to remove low frequency noise (including slow scanner drifts) and influences of higher frequencies reflecting cardiac and respiratory signals. Finally, similar to our previous study⁶², the data was smoothed using a full width half maximum of 6 mm.

Functional connectivity analysis for individual subjects was carried out in DPARSF by applying a seed-region approach using the left pmPFC ($x = 8$, $y = 40$, $z = 39$, with 5 mm radius) that showed significant cortical thickness difference between the real and sham acupuncture as seed (see Figure 1a). Next, the averaged time course was obtained from the seed and the correlation analysis was performed in a voxel-wise way to generate the FC map. The correlation coefficient map was converted into Fisher-Z map by Fisher's r -to- z transform to improve the normality by calling functions in REST.

To investigate the functional connectivity of left pmPFC at a group level, individual Fisher-Z functional connectivity maps obtained from the functional connectivity analysis in DPARSF were used in the second level analysis using SPM8 software (available at: <http://www.fil.ion.ucl.ac.uk/spm>).

To study the modulation effect of acupuncture treatment, we compared the changes in pre-acupuncture treatment 6 and pre-acupuncture treatment 1 in the verum group to that of the sham group. We used pre-acupuncture resting state fMRI to avoid the residual effect of acupuncture needle stimulation^{63,64}. Due to the small sample size of each group (10 patients), we decided to combine the two verum acupuncture groups (low and high dose groups) because 1) the total treatment time, needle stimulation time, and reported sensations were the same in both verum groups, and 2) we found no clinical outcome differences between the two verum acupuncture groups; both verum acupuncture groups trended towards improvement when compared to sham treatment.

Specifically, to explore the difference between verum and sham after longitudinal acupuncture treatments, we input individual Fisher-Z maps from FC analyses for each subject into a full factorial model with two factors. The first factor had two levels (high and low dose verum acupuncture, and sham acupuncture) and the second

factor had three levels (treatment 1, treatment 3, and treatment 6). Next, the contrast was created to look at the difference of differences, the first difference is FC changes between pre-acupuncture treatment 6 and pre-acupuncture treatment 1 for verum and sham acupuncture groups respectively, the second difference is FC changes between verum and sham group.

We used an initial threshold of $p < 0.005$ uncorrected with 10 voxels. We also report corrected p values as obtained from small volume correction in a priori regions of interest at a level of $p \leq 0.05$ with FWE peak correction. Coordinates for small volume correction were based on peak coordinates obtained from previous studies on pain processing and pain modulation. The PAG⁶⁵, the ventral striatum⁶² were corrected using spheres of 4 mm radius. The anterior MPFC⁶⁶ and the pregenual rostral anterior cingulate cortex (rACC)⁶⁷ were corrected using spheres of 9 mm radius.

Connectivity Fisher-Z values were extracted from areas surviving small volume correction for all groups and sessions. Repeated measurement was then performed using SPSS 18.0 Software to test for interaction between verum and sham group across treatment sessions. To eliminate the effect of possible confounding factors, all data analysis were repeated using age and duration as covariates of no interest.

Results

Forty-four acupuncture naive patients (19 females) aged 43–70 with a diagnosis of chronic osteoarthritis in the right and/or left knee participated in the study. Of the 44 patients who enrolled, 30 (13 females) completed all study procedures. Fourteen subjects did not complete the study due to problems with scheduling (6), ineligibility at screening (3), disinterest (2), claustrophobia (1), or inability to adhere to study requirements in scanner (2). Of the 14 subjects who dropped out of the study, four dropped out after randomization (2 from the low dose verum acupuncture group (one due to inability to adhere to study requirements in scanner, one due to schedule conflict) and 2 from the high dose verum acupuncture group (due to schedule conflict)).

Sensation evoked by acupuncture treatment. As a treatment quality control, we measured the deqi sensation evoked by acupuncture treatment using the Massachusetts General Hospital Acupuncture Sensation Scale (MASS)^{51,52}. The average total MASS score (sum of the intensities of each sensation) differed significantly across the acupuncture treatment groups (high (12.95 ± 7.55) vs. low (15.22 ± 11.90) vs. sham (4.82 ± 3.79)) ($F(2,27) = 4.21$, $p = .026$). Post hoc analyses showed the following differences: high vs low $p = 0.55$, high vs sham $p = 0.04$; low vs sham $p = 0.01$. These results indicate that verum acupuncture can produce significantly stronger sensations compared to sham acupuncture. There was no significant difference between the high and low dose acupuncture groups. A previous study by our group reported more details regarding the deqi sensations evoked by different treatment modalities in this sample⁵¹.

Clinical outcomes. Baseline characteristics for the 30 patients who completed all study procedures are detailed in Table 1. Two sample t -tests indicated no significant differences in clinical outcomes between the high and low dose groups for any of the KOOS subscale changes (post-treatment – pre-treatment) and both of the verum groups showed trends of improvements in the pain and other subscale scores when compared to the sham group (Table 2). Since the treatment duration and stimulation time, acupuncture needle-evoked sensation and the changes of clinical outcomes are similar between the high and low dose verum acupuncture groups, we pooled the data from these two groups to increase our power when comparing the differences between verum and sham acupuncture.

Repeated measurements show that there was a significant interaction between acupuncture mode (verum vs. sham) and time (baseline vs. endpoint) for pain ($F(1,28) = 5.596$, $p = .025$, significant after Bonferroni correction) and a trend for function in daily living ($F(1,28) = 3.223$, $p = .083$). In addition, we found that secondary outcomes (KOOS subscale score for function in sport ($F(1,27) = 4.252$, $p = .049$) and quality of life ($F(1, 28) = 4.682$, $p = .039$) showed significant improvement in the real acupuncture group after treatment compared to the sham group.


Table 1 | Clinical characteristics at baseline and after longitudinal acupuncture treatments

mean ± SD	All	High Dose	Low Dose	Sham
N (F)	30 (13)	10 (2)	10 (7)	10 (4)
Age	58 ± 8	60 ± 9	58 ± 8	54 ± 7
Duration (treated knee, years)*	11 ± 8	10 ± 7	6 ± 6	16 ± 8
Pain				
Baseline	56 ± 14	59 ± 13	53 ± 9	56 ± 19
Post-treatment	64 ± 14	70 ± 16	66 ± 11	56 ± 12
Symptoms				
Baseline	53 ± 16	57 ± 19	48 ± 11	54 ± 18
Post-treatment	58 ± 15	60 ± 20	58 ± 15	55 ± 11
Adjusted				
Baseline	64 ± 15	66 ± 12	61 ± 14	64 ± 20
Daily Living				
Post-treatment	72 ± 16	74 ± 18	76 ± 12	65 ± 15
Function in				
Baseline	30 ± 23	30 ± 18	31 ± 19 [†]	29 ± 31
Sport				
Post-treatment	41 ± 26	49 ± 33	48 ± 18	28 ± 21
Quality of Life				
Baseline	39 ± 15	42 ± 17	38 ± 14	36 ± 16
Post-treatment	38 ± 18	44 ± 20	41 ± 16	29 ± 17

Results reported as mean ± SD. Significant main effect of group (high vs. low vs. sham) indicated by *;

[†]indicates N = 9 due to one missing KOOS subscale score. Please be noted that greater score on the KOOS indicates improvement.

Cortical thickness analysis: comparing verum to sham group. Of all 30 subjects, 27 (9 in sham acupuncture group) have all brain structure data at three time points for analysis. Cluster analysis showed significant difference between the verum and sham acupuncture groups at left pMPFC (Figure 1a).

To further explore the cortical thickness change in different groups, we extracted the peak vertex of pMPFC in each subjects across three sessions. Results showed that the cortical thickness remained static for the verum group across all three treatments sessions, but decreased for sham group (Figure 1b). Repeated measurements on the extracted data show that there was a highly significant interaction between acupuncture mode (verum vs. sham) and time (across all three treatment sessions) for cortical thickness of left pMPFC ($F(2,24) = 7.519$, $p = 0.003$). After control for age and duration, the interaction remains significant ($F(2,22) = 7.461$, $p = 0.003$).

Functional connectivity: comparing verum to sham group. Using the left pMPFC that we obtained in structural analysis as a seed, we applied whole brain functional connectivity analysis comparing changes from pre-acupuncture treatment 1 to that of pre-acupuncture treatment 6 between the verum and sham groups. The FWE corrected P value, Fisher-Z value, and peak coordinates for all regions are shown in Table 3. There is significantly stronger connectivity between the left pMPFC and PAG, rACC, anterior MPFC and ventral striatum for verum acupuncture compared to sham acupuncture after longitudinal acupuncture treatment (Figure 2). When extracting the Fisher-Z connectivity values in these regions using the peak coordinates and a 4 mm sphere around the peak for all groups, repeated measurements show that there was a highly significant interaction between acupuncture mode

Table 2 | Two sample t-tests of KOOS subscale changes (post-treatment – pre-treatment) across three groups

Items	P value, High dose acu vs low dose acu	P value, High dose acu vs sham acu	P value, Low dose acu vs sham acu
KOOS pain	0.9	0.07	0.04
KOOS daily living	0.34	0.26	0.06
KOOS symptoms	0.26	0.71	0.13
KOOS sport	0.99	0.11	0.07
KOOS quality of life	1.0	0.11	0.06

Table 3 | Regions that show significant functional connectivity changes with left posterior MPFC after longitudinal acupuncture treatment (pre-treatment 6 – pre-treatment 1) comparing acupuncture to sham group

Brain Region	Fisher-Z value	Peak coordinate (x, y, z)
PAG	2.64	6, -30, -6
Right Ventral striatum	2.65	-12, 18, -3
Anterior MPFC	3.01	0, 60, -15
Pregenual ACC	3.03	6, 36, -18

(verum vs. sham) and time (across all three treatment sessions) for PAG ($F(2,27) = 8.637$, $p = 0.001$), rACC ($F(2,27) = 8.885$, $p = 0.001$), ventral striatum ($F(2,27) = 3.931$, $p = 0.032$), and anterior MPFC ($F(2,27) = 6.927$, $p = 0.004$). After using age and duration of the disorder as covariates of no interest, and repeat the analysis, all findings remain significant.

Discussion

In this study, we investigated the effects of longitudinal acupuncture treatment on structural and functional brain changes and clinical outcome measurements in knee OA patients. The results showed that acupuncture treatment can significantly modulate cortical thickness, functional connectivity, and clinical KOOS pain rating in OA patients.

Specifically, we found that the cortical thickness of left pMPFC decreased in sham group, but stayed the same in the verum group (Figure 1a,b). Previous studies^{68–70} have found the region involved in conditioning placebo analgesia. Literature⁷¹ suggest that the posterior region of the MPFC seems to be involved in control and monitoring of action. Other studies also suggest that the MPFC may integrate information from the external environment with stored internal representations⁷², control top-down attention during conflict processing of alternative responses⁷³, and control monitor conflict with subsequent adjustment in performance^{74–77}.

Cortical thickness, especially that of the frontal region, dramatically declines with age^{78–82}. Also, the cortical thinning process is accentuated in chronic pain population⁸³. Our result suggest that the acupuncture may have prevented the natural rapid cortical thinning process of Knee OA patients by increasing the ability of the left

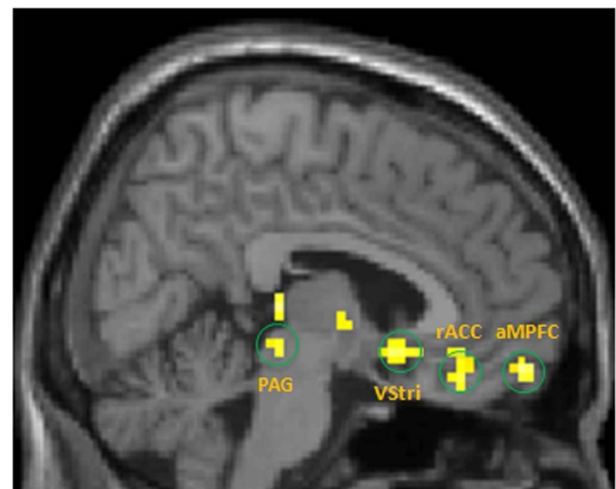


Figure 2 | The comparison in FC changes from pre-acupuncture treatment 1 to that of pre-acupuncture treatment 6 between the verum and sham groups indicates that the verum group showed stronger left posterior MPFC connectivity with periaqueductal grey (PAG), the anterior medial prefrontal cortex (aMPFC), rostral anterior cingulate cortex (rACC), and ventral striatum (VStri).



pMPFC to control and modulate one's pain experience, which ultimately decreased the subjects' experience of pain. We observed cortical thickness decrease after one month of treatment, which is comparable in change in brain structure and duration of treatment with other published results^{43,84,85}.

To further explore other brain areas involved in pain modulation, we used the left posterior MPFC obtained from cortical thickness change as a seed for functional connectivity analysis. We found that comparing resting state functional connectivity changes from pre-acupuncture treatment 1 to that of pre-acupuncture treatment 6 between the verum and sham groups, the verum group showed stronger left posterior MPFC connectivity with the PAG, the right ventral striatum, the anterior MPFC, and the pregenual part of rostral ACC than did the sham group after longitudinal acupuncture treatments (Figure 2). When extracting connectivity values from these regions and compared between verum and sham, there is significant interactions between verum and sham across all three sessions for all regions.

Diffusion tensor imaging showed that the pMPFC has strong anatomical and functional connections with the anterior MPFC and ACC⁸⁶. The MPFC/rACC (including the pre-genu and sub-genu ACC) is a key region involved in the descending pain modulatory system^{68,87–90}. Studies also have shown that in knee OA patients, the lateral prefrontal cortex, the rACC, the bilateral insula, the parietal operculum, and the limbic cortical areas are involved in altered pain processing in OA^{79,91}. This suggests that the MPFC/rACC is a main area involved in the OA pain circuit. It also forms a core network with the PAG and the RVM (ACC-PAG-RVM network) for pain modulation even in the absence of a painful stimulus⁹⁰. Recent studies have shown that the functional connectivity fluctuations and structural connectivity between the PAG and the rACC predicted the mind wandering away from pain⁶⁶.

Ventral striatum is involved in processing many types of rewards including analgesia. Studies have shown the role of ventral striatum/accumbens in anticipation of analgesia⁹². In a previous study, investigators found that the magnitude of opioid analgesia indicated by pain rating changes can be predicted by neuronal response to painful noxious stimuli in nucleus accumbens/ventral striatum before administration of remifentanyl⁹³. Taken together, these results highlight the role of reward network such as ventral striatum in opioid related pain modulation.

On top of the structural and functional connectivity changes, we also found that the verum group showed less clinical KOOS pain after acupuncture treatment compared with sham group, indicating acupuncture is an effective method at treating knee OA. In light of the above findings and previous studies^{14–16} on the mechanisms involved in acupuncture analgesia demonstrating the involvement of the pain descending modulatory system, we speculate that by maintaining the structural cortical thickness of the left pMPFC and the connectivity between the left pMPFC and the pregenual rACC, anterior MPFC, right ventral striatum and PAG, the communication between these regions stays intact, which further enhance the pleasantness of rewarding stimuli, and restore the descending modulatory pathway. The ultimate result is improved clinical outcome in knee OA patients.

There are several limitations of this study. First, the sample size is relatively small. However, by combining the two acupuncture groups, we increased the power of the verum group, creating a 2:1 ratio between the verum and sham treatment conditions that will provide additional information on patients receiving active treatment⁹⁴. All reported main brain imaging results survived the stringent multiple comparison correction. Due to the longitudinal design of the study, we acquired fMRI scans at three time points, which may also increase the power of this study.

Other potential limitations of this study include the potentially confounding effect of factors such as patient age and duration of

chronic pain experienced by each patient. To address this concern, we repeated the analysis including age and duration of pain as covariates of no interest and re-analyzed the data. After this analysis, all findings remain significant. Thus, our main results do not change after controlling for these confounding factors. Furthermore, when KOOS pain scores were correlated with age and duration using multiple regression, we did not find any significant correlation. Further studies that include larger sample sizes are needed to validate the findings from our study. Finally, 6 minutes resting fMRI scans may potentially influence the test-retest reliability of seed based functional connectivity result. A longer duration of resting state scan should be applied in future study⁹⁵.

Conclusion

In this study, we found that verum acupuncture treatment can significantly modulate cortical thickness change, clinical outcome changes and FC associated with chronic pain in knee OA patients. Our findings suggest that verum acupuncture may enhance connectivity in the descending pain modulation pathway through connection with the posterior MPFC. A better understanding of the association in structural changes, FC and clinical outcomes and how treatment can modulate FC will deepen our knowledge and may ultimately lead to the acceptance of acupuncture in the mainstream medicine and the development of mechanism-based therapies for treating chronic pain.

1. Ho-Pham, L. T. *et al.* Prevalence of radiographic osteoarthritis of the knee and its relationship to self-reported pain. *PLoS One* **9**, e94563, doi:10.1371/journal.pone.0094563 PONE-D-13-46418 (2014).
2. Nguyen, U. S. *et al.* Increasing prevalence of knee pain and symptomatic knee osteoarthritis: survey and cohort data. *Ann Intern Med* **155**, 725–732, doi:155/11/725 10.7326/0003-4819-155-11-201112060-00004 (2011).
3. Hochman, J. R., Davis, A. M., Elkayam, J., Gagliese, L. & Hawker, G. A. Neuropathic pain symptoms on the modified painDETECT correlate with signs of central sensitization in knee osteoarthritis. *Osteoarthritis Cartilage* **21**, 1236–1242, doi:S1063-4584(13)00859-5 10.1016/j.joca.2013.06.023 (2013).
4. Arendt-Nielsen, L. *et al.* Sensitization in patients with painful knee osteoarthritis. *Pain* **149**, 573–581 (2010).
5. Finan, P. H. *et al.* Discordance between pain and radiographic severity in knee osteoarthritis: findings from quantitative sensory testing of central sensitization. *Arthritis Rheum* **65**, 363–372, doi:10.1002/art.34646 (2013).
6. Gwilym, S. E. *et al.* Psychophysical and functional imaging evidence supporting the presence of central sensitization in a cohort of osteoarthritis patients. *Arthritis Rheum* **61**, 1226–1234 (2009).
7. Howard, M. A. *et al.* Alterations in resting-state regional cerebral blood flow demonstrate ongoing pain in osteoarthritis: An arterial spin-labeled magnetic resonance imaging study. *Arthritis Rheum* **64**, 3936–3946, doi:10.1002/art.37685 (2012).
8. Gay, M. C., Philippot, P. & Luminet, O. Differential effectiveness of psychological interventions for reducing osteoarthritis pain: a comparison of Erickson [correction of Erickson] hypnosis and Jacobson relaxation. *Eur J Pain* **6**, 1–16, doi:10.1053/eujp.2001.0263 S1090380101903143 (2002).
9. Berman, B. M. *et al.* Effectiveness of acupuncture as adjunctive therapy in osteoarthritis of the knee: a randomized, controlled trial. *Ann Intern Med* **141**, 901–910 (2004).
10. Felson, D. T. *et al.* Osteoarthritis: new insights. Part 2: treatment approaches. *Ann Intern Med* **133**, 726–737 (2000).
11. Witt, C. *et al.* Acupuncture in patients with osteoarthritis of the knee: a randomised trial. *Lancet* **366**, 136–143 (2005).
12. Scharf, H. P. *et al.* Acupuncture and knee osteoarthritis: a three-armed randomized trial. *Ann Intern Med* **145**, 12–20 (2006).
13. Mavrommatis, C. I., Argyra, E., Vadalouka, A. & Vasilakos, D. G. Acupuncture as an adjunctive therapy to pharmacological treatment in patients with chronic pain due to osteoarthritis of the knee: a 3-armed, randomized, placebo-controlled trial. *Pain* **153**, 1720–1726 (2012).
14. Han, J. S. Acupuncture analgesia: areas of consensus and controversy. *Pain* **152**, S41–48 (2011).
15. Hans, J. S. Physiology of acupuncture: review of thirty years of research. *J Altern Complement Med (Suppl 1)*, S101–108 (1997).
16. Zhao, Z. Q. Neural mechanism underlying acupuncture analgesia. *Prog Neurobiol* **85**, 355–375 (2008).
17. Chae, Y. *et al.* Inserting needles into the body: a meta-analysis of brain activity associated with acupuncture needle stimulation. *J Pain* **14**, 215–222 (2013).



18. Huang, W. *et al.* Characterizing acupuncture stimuli using brain imaging with fMRI—a systematic review and meta-analysis of the literature. *PLoS One* **7**, e32960 (2012).
19. Kong, J. *et al.* Test-retest study of fMRI signal change evoked by electroacupuncture stimulation. *Neuroimage* **34**, 1171–1181 PMID: PMC1994822 (2007).
20. Leung, A., Zhao, Y. & Shukla, S. The effect of acupuncture needle combination on central pain processing—an fMRI study. *Mol Pain* **10**, 23, doi:1744-8069-10-23 (2014).
21. Kong, J. *et al.* A pilot study of functional magnetic resonance imaging of the brain during manual and electroacupuncture stimulation of acupuncture point (LI-4 Hegu) in normal subjects reveals differential brain activation between methods. *J Altern Complement Med* **8**, 411–419 (2002).
22. Zyloney, C. E. *et al.* Imaging the functional connectivity of the Periaqueductal Gray during genuine and sham electroacupuncture treatment. *Mol Pain* **6**, 80 (2010).
23. Dhond, R. P., Yeh, C., Park, K., Kettner, N. & Napadow, V. Acupuncture modulates resting state connectivity in default and sensorimotor brain networks. *Pain* **136**, 407–418 (2008).
24. Liu, P. *et al.* Combining spatial and temporal information to explore function-guide action of acupuncture using fMRI. *J Magn Reson Imaging* **30**, 41–46 (2009).
25. Bai, L. *et al.* Acupuncture modulates spontaneous activities in the anticorrelated resting brain networks. *Brain Res* **1279**, 37–49, doi:S0006-8993(09)00899-3 (2009).
26. Qin, W. *et al.* fMRI connectivity analysis of acupuncture effects on an amygdala-associated brain network. *Mol Pain* **4**, 55 (2008).
27. Liu, B. *et al.* Altered small-world efficiency of brain functional networks in acupuncture at ST36: a functional MRI study. *PLoS One* **7**, e39342, doi:10.1371/journal.pone.0039342 PONE-D-11-22310 (2012).
28. Sun, R. *et al.* Connectomics: A New Direction in Research to Understand the Mechanism of Acupuncture. *Evid Based Complement Alternat Med* **2014**, 568429, doi:10.1155/2014/568429 (2014).
29. Zhang, Y. *et al.* An fMRI study of acupuncture using independent component analysis. *Neurosci Lett* **449**, 6–9, doi:S0304-3940(08)01450-X 10.1016/j.neulet.2008.10.071 (2009).
30. Apkarian, A. V. *et al.* Chronic back pain is associated with decreased prefrontal and thalamic gray matter density. *J Neurosci* **24**, 10410–10415 (2004).
31. Flor, H. Cortical reorganisation and chronic pain: implications for rehabilitation. *J Rehabil Med* **41 Suppl**, 66–72 (2003).
32. Schmidt-Wilcke, T. *et al.* Affective components and intensity of pain correlate with structural differences in gray matter in chronic back pain patients. *Pain* **125**, 89–97 (2006).
33. Baliki, M. N., Schnitzer, T. J., Bauer, W. R. & Apkarian, A. V. Brain morphological signatures for chronic pain. *PLoS One* **6**, e26010 (2011).
34. May, A. Chronic pain may change the structure of the brain. *Pain* **137**, 7–15 (2008).
35. Henry, D. E., Chiodo, A. E. & Yang, W. Central nervous system reorganization in a variety of chronic pain states: a review. *Pm R* **3**, 1116–1125 (2011).
36. Kong, J. *et al.* S1 is associated with chronic low back pain: a functional and structural MRI study. *Molecular pain* **9**, doi:10.1186/1744-8069-1189-1143 (2013).
37. Jensen, K. *et al.* Overlapping structural and functional brain changes in patients with long-term exposure to fibromyalgia. *Arthritis & Rheumatism* **65**, 3293–3303 (2013).
38. Apkarian, A. V., Baliki, M. N. & Geha, P. Y. Towards a theory of chronic pain. *Prog Neurobiol* **87**, 81–97 (2009).
39. Bushnell, M. C. How neuroimaging studies have challenged us to rethink: is chronic pain a disease? *J Pain* **10**, 1113–1120 (2009).
40. Davis, K. D. & Moayedi, M. Central Mechanisms of Pain Revealed Through Functional and Structural MRI. *J Neuroimmune Pharmacol* **8**, 518–534 (2013).
41. Baliki, M. N. *et al.* Corticostriatal functional connectivity predicts transition to chronic back pain. *Nat Neurosci*, doi:10.1038/nn.3153 (2012).
42. Loggia, M. L. *et al.* Default mode network connectivity encodes clinical pain: An arterial spin labeling study. *Pain* **154**, 24–33 (2013).
43. Seminowicz, D. A. *et al.* Effective treatment of chronic low back pain in humans reverses abnormal brain anatomy and function. *J Neurosci* **31**, 7540–7550 (2011).
44. Gwilym, S. E., Filippini, N., Douaud, G., Carr, A. J. & Tracey, I. Thalamic atrophy associated with painful osteoarthritis of the hip is reversible after arthroplasty: a longitudinal voxel-based morphometric study. *Arthritis Rheum* **62**, 2930–2940 (2010).
45. Roos, E. M. & Toksvig-Larsen, S. Knee injury and Osteoarthritis Outcome Score (KOOS) – validation and comparison to the WOMAC in total knee replacement. *Health and Quality of Life Outcomes* **1**, 1–10 (2003).
46. Cheng, X. N. *Chinese acupuncture and moxibustion*. (Foreign Language Press, 1987).
47. Streitberger, K. & Kleinhenz, J. Introducing a placebo needle into acupuncture research. *Lancet* **352**, 364–365 (1998).
48. Kong, J. *et al.* Psychophysical outcomes from a randomized pilot study of manual, electro, and sham acupuncture treatment on experimentally induced thermal pain. *J Pain* **6**, 55–64 (2005).
49. Kong, J. *et al.* Brain activity associated with expectancy-enhanced placebo analgesia as measured by functional magnetic resonance imaging. *J Neurosci* **26**, 381–388 (2006).
50. Zhu, D., Gao, Y., Chang, J. & Kong, J. Placebo acupuncture devices: considerations for acupuncture research. *Evid Based Complement Alternat Med* **2013**, 628907 (2013).
51. Spaeth, R. B. *et al.* A longitudinal study of the reliability of acupuncture deqi sensations in knee osteoarthritis. *Evid Based Complement Alternat Med* **2013**, 204259 (2013).
52. Kong, J. *et al.* Acupuncture de qi, from qualitative history to quantitative measurement. *J Altern Complement Med* **13**, 1059–1070 (2007).
53. Dale, A. M., Fischl, B. & Sereno, M. I. Cortical surface-based analysis. I. Segmentation and surface reconstruction. *Neuroimage* **9**, 179–194 (1999).
54. Fischl, B. *et al.* Whole brain segmentation: automated labeling of neuroanatomical structures in the human brain. *Neuron* **33**, 341–355 (2002).
55. Fischl, B., Sereno, M. I. & Dale, A. M. Cortical surface-based analysis. II: Inflation, flattening, and a surface-based coordinate system. *Neuroimage* **9**, 195–207 (1999).
56. Reuter, M., Schmansky, N. J., Rosas, H. D. & Fischl, B. Within-subject template estimation for unbiased longitudinal image analysis. *Neuroimage* **61**, 1402–1418, doi:S1053-8119(12)00276-5 10.1016/j.neuroimage.2012.02.084 (2012).
57. Reuter, M. & Fischl, B. Avoiding asymmetry-induced bias in longitudinal image processing. *Neuroimage* **57**, 19–21, doi:S1053-8119(11)00253-9 10.1016/j.neuroimage.2011.02.076 (2011).
58. Reuter, M., Rosas, H. D. & Fischl, B. Highly accurate inverse consistent registration: a robust approach. *Neuroimage* **53**, 1181–1196, doi:S1053-8119(10)00971-7 10.1016/j.neuroimage.2010.07.020 (2010).
59. Chao-Gan, Y. & Yu-Feng, Z. DPARSF: A MATLAB Toolbox for “Pipeline” Data Analysis of Resting-State fMRI. *Front Syst Neurosci* **4**, 13 (2010).
60. Yan, C. G. *et al.* A comprehensive assessment of regional variation in the impact of head micromovements on functional connectomics. *Neuroimage* **76**, 183–201, doi:S1053-8119(13)00212-7 10.1016/j.neuroimage.2013.03.004 (2013).
61. Song, X. W. *et al.* REST: a toolkit for resting-state functional magnetic resonance imaging data processing. *PLoS One* **6**, e25031, doi:10.1371/journal.pone.0025031 PONE-D-11-09456 (2011).
62. Yu, R. *et al.* Placebo analgesia and reward processing: Integrating genetics, personality, and intrinsic brain activity. *Hum Brain Mapp*, doi: 10.1002/hbm.22496 (2014).
63. Bai, L. *et al.* Time-varied characteristics of acupuncture effects in fMRI studies. *Hum Brain Mapp* **30**, 3445–3460, doi:10.1002/hbm.20769 (2009).
64. Bai, L. *et al.* Acupuncture modulates temporal neural responses in wide brain networks: evidence from fMRI study. *Mol Pain* **6**, 73, doi:1744-8069-6-73 (2010).
65. Fairhurst, M., Wiech, K., Dunckley, P. & Tracey, I. Anticipatory brainstem activity predicts neural processing of pain in humans. *Pain* **128**, 101–110, doi:S0304-3959(06)00458-1 10.1016/j.pain.2006.09.001 (2007).
66. Kucyi, A., Salomons, T. V. & Davis, K. D. Mind wandering away from pain dynamically engages antinociceptive and default mode brain networks. *Proc Natl Acad Sci U S A* **110**, 18692–18697, doi:1312902110 10.1073/pnas.1312902110 (2013).
67. Bingel, U., Schoell, E., Herken, W., Buchel, C. & May, A. Habituation to painful stimulation involves the antinociceptive system. *Pain* **131**, 21–30, doi:S0304-3959(06)00670-1 10.1016/j.pain.2006.12.005 (2007).
68. Kong, J. *et al.* Functional connectivity of frontoparietal network predicts cognitive modulation of pain. *Pain* **154**, 459–467 (2013).
69. Lui, F. *et al.* Neural bases of conditioned placebo analgesia. *Pain* **151**, 816–824 (2010).
70. Atlas, L. Y., Bolger, N., Lindquist, M. A. & Wager, T. D. Brain mediators of predictive cue effects on perceived pain. *J Neurosci* **30**, 12964–12977 (2010).
71. Amodio, D. M. & Frith, C. D. Meeting of minds: the medial frontal cortex and social cognition. *Nat Rev Neurosci* **7**, 268–277, doi:nrn1884 10.1038/nrn1884 (2006).
72. Miller, E. K. The prefrontal cortex and cognitive control. *Nat Rev Neurosci* **1**, 59–65 (2000).
73. Corbetta, M. & Shulman, G. L. Control of goal-directed and stimulus-driven attention in the brain. *Nat Rev Neurosci* **3**, 201–215 (2002).
74. Ridderinkhof, K. R., Ullsperger, M., Crone, E. A. & Nieuwenhuis, S. The role of the medial frontal cortex in cognitive control. *Science* **306**, 443–447 (2004).
75. Matsumoto, K. & Tanaka, K. Neuroscience. Conflict and cognitive control. *Science* **303**, 969–970 (2004).
76. Carter, C. S. & van Veen, V. Anterior cingulate cortex and conflict detection: an update of theory and data. *Cogn Affect Behav Neurosci* **7**, 367–379 (2007).
77. Crone, E. A., Wendelken, C., Donohue, S. E. & Bunge, S. A. Neural evidence for dissociable components of task-switching. *Cereb Cortex* **16**, 475–486 (2006).
78. Sowell, E. R. *et al.* Mapping cortical change across the human life span. *Nat Neurosci* **6**, 309–315, doi:10.1038/nn1008 nn1008 (2003).
79. Fjell, A. M. *et al.* High consistency of regional cortical thinning in aging across multiple samples. *Cereb Cortex* **19**, 2001–2012, doi:bhn232 10.1093/cercor/bhn232 (2009).
80. Salat, D. H. *et al.* Thinning of the cerebral cortex in aging. *Cereb Cortex* **14**, 721–730, doi:10.1093/cercor/bhh032 bhh032 (2004).
81. Thompson, P. M. *et al.* Mapping cortical change in Alzheimer’s disease, brain development, and schizophrenia. *Neuroimage* **23 Suppl 1**, S2–18, doi:S1053-8119(04)00399-4 10.1016/j.neuroimage.2004.07.071 (2004).



82. Jernigan, T. L. *et al.* Effects of age on tissues and regions of the cerebrum and cerebellum. *Neurobiol Aging* **22**, 581–594, doi:S0197458001002172 (2001).
83. Chong, C. D., Dodick, D. W., Schlaggar, B. L. & Schwedt, T. J. Atypical age-related cortical thinning in episodic migraine. *Cephalalgia*, doi:0333102414531157 10.1177/0333102414531157 (2014).
84. Tang, Y. Y., Lu, Q., Fan, M., Yang, Y. & Posner, M. I. Mechanisms of white matter changes induced by meditation. *Proc Natl Acad Sci U S A* **109**, 10570–10574, doi:1207817109 10.1073/pnas.1207817109 (2012).
85. Engvig, A. *et al.* Effects of memory training on cortical thickness in the elderly. *Neuroimage* **52**, 1667–1676, doi:S1053-8119(10)00773-1 10.1016/j.neuroimage.2010.05.041 (2010).
86. Liu, H. *et al.* Connectivity-based parcellation of the human frontal pole with diffusion tensor imaging. *J Neurosci*, **16**, 6782–90 (2013).
87. Fields, H. State-dependent opioid control of pain. *Nat Rev Neurosci* **5**, 565–575 (2004).
88. Tracey, I. *et al.* Imaging attentional modulation of pain in the periaqueductal gray in humans. *J Neurosci* **22**, 2748–2752 (2002).
89. Jensen, K. B. *et al.* Patients With Fibromyalgia Display Less Functional Connectivity In The Brain's Pain Inhibitory Network. *Mol Pain* **8**, 32 (2012).
90. Kong, J., Tu, P. C., Zyloney, C. & Su, T. P. Intrinsic functional connectivity of the periaqueductal gray, a resting fMRI study. *Behav Brain Res* **211**, 215–219 (2010).
91. Parks, E. L. *et al.* Brain activity for chronic knee osteoarthritis: dissociating evoked pain from spontaneous pain. *Eur J Pain* **15**, 843 e841–814, doi:S1090-3801(11)00019-X 10.1016/j.ejpain.2010.12.007 (2011).
92. Scott, D. J. *et al.* Individual differences in reward responding explain placebo-induced expectations and effects. *Neuron* **55**, 325–336 (2007).
93. Wanigasekera, V. *et al.* Baseline reward circuitry activity and trait reward responsiveness predict expression of opioid analgesia in healthy subjects. *Proc Natl Acad Sci U S A* **109**, 17705–17710, doi:1120201109 10.1073/pnas.1120201109 (2012).
94. Dumville, J., Hahn, S., Miles, J. & Torgerson, D. The use of unequal randomisation ratios in clinical trials: A review. *Contemporary Clinical Trials* **27**, 1–12 (2006).
95. Zuo, X. N. & Xing, X. X. Test-retest reliabilities of resting-state FMRI measurements in human brain functional connectomics: A systems neuroscience perspective. *Neurosci Biobehav Rev* **45C**, 100–118, doi:S0149-7634(14)00126-2 10.1016/j.neubiorev.2014.05.009 (2014).

Acknowledgments

This work was supported by R21AT004497 (NCCAM), R03AT218317 (NIDA), R01AT006364 (NCCAM) to Jian Kong, R01AT005280 (NCCAM) to Randy Gollub, and P01 AT006663 to Bruce Rosen. There is no conflict of interest for any of the authors. We thank Dr. Martin Reuter from Martino center at Massachusetts General Hospital for his technique support.

Author contributions

X.Y.C.: data analysis and manuscript preparation; R.B.S.: data collection, data analysis and manuscript preparation; K.R.: data analysis; D.O.: manuscript preparation; J.K.: experimental design, data collection, analysis and manuscript preparation.

Additional information

Clinical Trial Registration URL: <http://clinicaltrials.gov>. Unique identifier: NCT01079390

Supplementary information accompanies this paper at <http://www.nature.com/scientificreports>

Competing financial interests: The authors declare no competing financial interests.

How to cite this article: Chen, X., Spaeth, R.B., Retzepi, K., Ott, D. & Kong, J. Acupuncture modulates cortical thickness and functional connectivity in knee osteoarthritis patients. *Sci Rep.* **4**, 6482; DOI:10.1038/srep06482 (2014).



This work is licensed under a Creative Commons Attribution-NonCommercial-NoDerivs 4.0 International License. The images or other third party material in this article are included in the article's Creative Commons license, unless indicated otherwise in the credit line; if the material is not included under the Creative Commons license, users will need to obtain permission from the license holder in order to reproduce the material. To view a copy of this license, visit <http://creativecommons.org/licenses/by-nc-nd/4.0/>